2013 European Control Conference (ECC)
July 17-19, 2013, Zürich, Switzerland.

Sliding-Mode Control of a Hydrostatic Drive Train with Uncertain Actuator Dynamics

Hao Sun and Harald Aschemann

***Abstract*— A sliding-mode approach with disturbance compensation is proposed in this paper for the tracking control of a hydrostatic drive train, which is commonly used in off-road vehicles. A control-oriented modelling results in a system of four nonlinear differential equations which are subject to uncertain actuator dynamics with saturation effects and unknown disturbances – a leakage volume flow and a disturbance torque acting on the hydraulic motor. The disturbances are estimated by a nonlinear reduced-order disturbance observer and used for a disturbance compensation. Thereby, the switching part in the sliding-mode control law and chattering phenomena can be reduced. Simulation results point out that the proposed approach leads to an excellent tracking performance despite the given uncertainties in the actuator dynamics.**

I. Introduction

A hydrostatic transmission uses hydraulic oil to transmit power from the power source to the drive mechanism [1]. A simple hydrostatic transmission consists of a hydraulic pump and a hydraulic motor, of which at least one must have a variable displacement, operating together in a closed circuit. The fluid flows directly from the motor outlet to the pump inlet, without returning to the tank. On the pump side the mechanical torque from the engine is transformed by the hydraulic pump into a pressurised fluid flow which is transformed back to mechanical torque by the hydraulic motor. By varying the tilt angle (changing the displacement) of either pump or motor, any desired transmission ratio can be obtained within a predefined boundary.

Hydrostatic transmissions are widely used as a characteristic component of drive trains in practically all types of working machines like harvesters, wheel loaders, excavators, telehandlers and agricultural tractors. They are typically operated in combination with diesel engines for mobile applications and offer a variety of advantages in comparison to pure mechanical transmissions. Besides the capability of a continuously variable transmission with high power density and the generation of large traction forces at low speeds, hydrostatic transmissions allow for reversing the direction of rotation without changing the gear. Moreover, it is possible to perform breaking manoeuvres without mechanical wear. Due to the significant advantages in comparison with mechanical gearboxes, hydrostatic transmissions have also attracted the attention of engineers from other industrial fields like wind energy technology in [2], [3], and [4].

Hydrostatic transmission systems are subject to several nonlinearities due to input saturation, friction, directional change of the valve opening, unknown load and leakage, which complicates a model-based control of such a system. Even so, gain-scheduled PID-controllers are still currently the choice of industrial practice for controlling hydrostatic transmissions [5]. In order to improve energy efficiency and to consider environmental aspects in mobile applications, a model-based nonlinear control approach has been proposed in [6], [7]. Both the simulation and experimental results show that the approach can lead to higher tracking accuracy and active damping of pressure oscillations. Additional uncertainty due to an unknown load torque acting on the motor side is considered and counteracted by an observer-based disturbance compensation. The control approach discussed in [6], [7] is based on the assumption that an approximate feedforward compensation of the known actuator dynamics can be achieved, which leads to a model order reduction. In this case, only the difference pressure and motor angular velocity are used for feedback control.

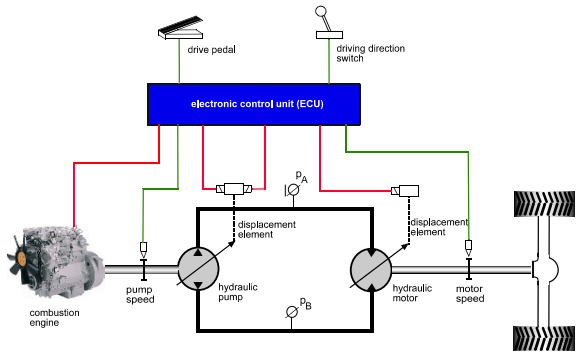

Fig. 1. Drive train with a closed-circuit hydrostatic transmission.

Considering both uncertainty in the actuator dynamics – imperfectly known time constants in the actuator dynamics – and unknown disturbances – a leakage volume flow as well as a load torque acting on the hydraulic motor – a sliding-mode controller with disturbance observer is proposed in this paper. Sliding-mode control uses a high frequency switching control action to bring the trajectories in finite time to a predefined sliding surface and keep them within the vicinity of this surface thereafter. Sliding-mode control has been known as a standard approach to tackle parametric uncertainties, although it has been subject to problems in applications regarding chattering phenomena [8], [9] and [10]. The paper is organised as follows: in Sec. II, the control-oriented modelling of the hydrostatic drive train system depicted in Fig. 1 is addressed. A sliding-mode controller is designed for the

Hao Sun and Harald Aschemann are with the Chair of Mechatronics, University of Rostock, Germany. {Hao.Sun, Harald.Aschemann}@uni-rostock.de

hydrostatic drive train considering explicitly the uncertainties in the actuators in Sec. III. In Sec. IV, a reduced-order disturbance observer is introduced. The estimated leakage volume flow and the disturbance torque can then be used for compensation measures in the control scheme. At control allocation, the displacement limitation due to physically bounded tilt angle at both pump and motor is also considered in this paper. The simulation results presented in Sec. V show excellent tracking performance for both the difference pressure and the motor angular velocity.

II. Control-Oriented Modelling

Dynamic system modelling plays a dominant role in modern control technology. An accurate system model is the key to improving the overall system performance. The considered mechatronic system is divided into a hydraulic subsystem and a mechanical subsystem, which are coupled by the torque generated by the hydraulic motor [11].

A. Hydraulic subsystem

The hydraulic pump is connected to the rotor shaft, and its main function is to convert mechanical energy into hydraulic energy. Pumps are characterized by a volumetric displacement V_p in $\mathrm{m}^3/\mathrm{rev}$, which describes the fluid volume displaced per rotation of the rotor shaft. The pump flow q_p is determined by a nonlinear function $q_P = V_P(\alpha_P)n_P$. The calculation of the pump volumetric displacement depends on the specific mechanical design. For the widely used axial piston pump with a tiltable swashplate, V_P can be expressed as

$$V_P(\alpha_P) = N_P A_P d_P \tan(\alpha_{P,max} \cdot \tilde{\alpha}_P). \tag{1}$$

Here, $\alpha_P = \alpha_{P,max} \cdot \tilde{\alpha}_P$ denotes the swashplate angle of the pump, A_P the effective piston area, d_P the diameter of the piston circle, and N_P the number of pistons. With the reasonable assumption of a small swashplate angle $|\alpha_P| \leq 18°$ [12], and

$$\tilde{V}_P = \frac{N_P A_P d_P \alpha_{P,max}}{2\pi}, \tag{2}$$

the pump volume flow can be described by $q_P = \tilde{V}_P \tilde{\alpha}_P \omega_P$. Here, the normalized swashplate angle $\tilde{\alpha}_P \in (-1, 1)$ and the rotational speed of pump ω_P are introduced. Accordingly, the volume flow rate $q_M = V_M(\alpha_M)n_M$ into the hydraulic motor can be formulated as a nonlinear function of the bent axis angle, with

$$V_M(\alpha_M) = N_M A_M d_M \sin(\alpha_{M,max} \cdot \tilde{\alpha}_M). \tag{3}$$

As before, the assumption of a small tilt angle $\alpha_M \leq 20°$ and

$$\tilde{V}_M = \frac{N_M A_M d_M \alpha_{M,max}}{2\pi} \tag{4}$$

allow for a simplified relationship $q_M = \tilde{V}_M \tilde{\alpha}_M \omega_M$, with the normalized angle $\tilde{\alpha}_M \in (\epsilon_M, 1)$, $\epsilon_M > 0$, and the motor angular velocity ω_M. Without consideration of the pressure loss in the transmission lines, the high- and low-pressure side can be described by one pressure value p_A and p_B, respectively. The pressure dynamics of the hydrostatic

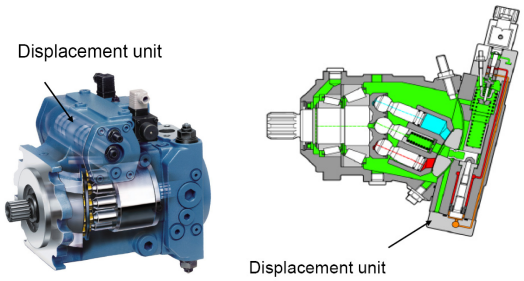

Fig. 2. Axial piston hydraulic pump (left, swashplate design) as well as hydraulic motor (right, bent axis design).

transmission in closed-loop configuration follows from a mass balance in combination with an oil model [12]

$$\dot{p}_A = \frac{\beta_A}{V_A}(q_P - q_M - q_{IL} - q_{ELA}), \tag{5}$$

$$\dot{p}_B = \frac{\beta_B}{V_B}(-q_P + q_M + q_{IL} - q_{ELB}). \tag{6}$$

Here, β_k, $k \in \{A, B\}$, denotes the effective bulk modulus of the fluid, and V_k describes the volume of the corresponding transmission line. The internal leakage oil flow q_{IL} is modelled as a laminar flow resistance [1], which depends linearly on the difference pressure

$$q_{IL} = k_{IL} \cdot (p_A - p_B) \tag{7}$$

and is characterized by the leakage coefficient k_{IL}. The external leakage can be described by [12]

$$q_{ELA} = k_{ELA} \cdot p_A, \tag{8}$$

$$q_{ELB} = k_{ELB} \cdot p_B. \tag{9}$$

Here, k_{ELA} and k_{ELB} represent the external leakage coefficients. A model order reduction becomes possible, if some reasonable symmetry assumptions are made. Considering identical capacitances $C_A = C_B =: C_H$, see [1] and [13], with

$$C_H = \frac{V_k}{\beta_k}, \; k \in \{A, B\} \tag{10}$$

leads to an order reduction by one. As a result, the differential equation for the difference pressure is given by

$$\Delta\dot{p} = \frac{2}{C_H}\left(\tilde{V}_P \, \tilde{\alpha}_P \omega_P - \tilde{V}_M \, \tilde{\alpha}_M \omega_M - \frac{q_U}{2}\right), \tag{11}$$

with a resulting leakage volume flow

$$q_U = 2k_{IL}\Delta p + k_{ELA}\, p_A - k_{ELB}\, p_B. \tag{12}$$

as a lumped disturbance. The dynamics of the displacement units for both pump and motor is characterised by a first-order lag behaviour, respectively, according to

$$T_{ui}\, \dot{\tilde{\alpha}}_i + \tilde{\alpha}_i = u_i, \; i \in \{P, M\}, \tag{13}$$

where the time constants T_{ui} are not exactly known and uncertain. The input voltages u_i of the corresponding proportional valves for the displacement units serve as physical control inputs. As the tilt angles of the diplacements units

are limited, saturation functions $\mathrm{sat}_b^a(\tilde{\alpha}_i)$ are introduced as follows

$$\mathrm{sat}_b^a(\tilde{\alpha}_i) = \begin{cases} \tilde{\alpha}_{i,max} & \tilde{\alpha}_i \geq a \\ \tilde{\alpha}_i \quad \text{for} & b < \tilde{\alpha}_i < a\,, \\ \tilde{\alpha}_{i,min} & \tilde{\alpha}_i \leq b \end{cases} \tag{14}$$

where $a = \tilde{\alpha}_{i,max}$ and $b = \tilde{\alpha}_{i,min}$ represent the upper and lower output limits determined by the mechanical design: $\{\epsilon_M, 1\}$ for the hydraulic motor and $\{-1, 1\}$ for the hydraulic pump. In the simulation model, (13) is implemented with limited integrators for $\tilde{\alpha}_P$ and $\tilde{\alpha}_M$.

B. Mechanical subsystem

The longitudinal dynamics of the working machine is governed by the equation of motion. The vehicle with the drive train (vehicle mass m_v, wheel radius r_w, gear box transmission ratio i_g, rear axle transmission ratio i_a, damping coefficient d_g at the drive shaft), see also Fig. 3, can be described by the following first order differential equation

$$\underbrace{\left(J_M + \frac{J_g}{i_g{}^2} + \frac{J_a + m_V\, r_w^2}{i_a^2\, i_g^2}\right)}_{J_V} \dot{\omega}_M + \underbrace{\frac{d_g}{i_g^2}}_{d_V} \omega_M = \tag{15}$$

$$\underbrace{\tilde{V}_M \Delta p\, \tilde{\alpha}_M}_{\tau_M} - \underbrace{\left(\tau_{Mf} \tanh(\frac{\omega_M}{\varepsilon}) + \tau_{gf} \tanh(\frac{\omega_M}{i_g \varepsilon}) + \frac{\tau_L}{i_a i_g}\right)}_{\tau_U},$$

where τ_M is the torque of the hydraulic motor. J_M, J_g and J_a are the mass moments of inertia of the hydraulic motor, gear box and rear axle, respectively. The maximum values τ_{Mf} and τ_{gf} characterise the friction models of the hydraulic motor and the gear box, whereas $\varepsilon << 1$ represents a small number.

C. State-space description

The overall system model involves four first order differential equations. Introducing the normalized angles of the displacement units $\tilde{\alpha}_i$, $i \in \{P, M\}$, the difference pressure Δp, and the motor angular velocity ω_M as state variables, the state vector results in $\mathbf{x} = [\tilde{\alpha}_P, \tilde{\alpha}_M, \Delta p, \omega_M]^T$. The corresponding state-space representation becomes

$$\begin{bmatrix} \dot{\tilde{\alpha}}_P \\ \dot{\tilde{\alpha}}_M \\ \Delta\dot{p} \\ \dot{\omega}_M \end{bmatrix} = \begin{bmatrix} -\frac{1}{T_{uP}}\tilde{\alpha}_P + \frac{1}{T_{uP}} u_P \\ -\frac{1}{T_{uM}}\tilde{\alpha}_M + \frac{1}{T_{uM}} u_M \\ \frac{2\tilde{V}_P \omega_P}{C_H} \mathrm{sat}_{-1}^{1}(\tilde{\alpha}_P) - \frac{2\tilde{V}_M \omega_M}{C_H} \mathrm{sat}_{\epsilon_M}^{1}(\tilde{\alpha}_M) - \frac{q_U}{C_H} \\ -\frac{d_V}{J_V}\omega_M + \frac{\tilde{V}_M}{J_V} \Delta p\, \mathrm{sat}_{\epsilon_M}^{1}(\tilde{\alpha}_M) - \frac{\tau_U}{J_V} \end{bmatrix}. \tag{16}$$

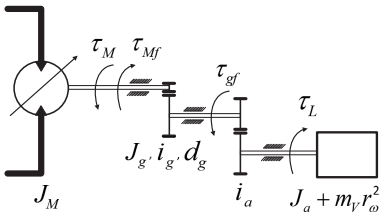

Fig. 3. Kinematical structure of the drive train with gear boxes and disturbance torque.

III. Sliding-Mode control Design

A sliding-mode controller is derived in this section. The control scheme of the whole dynamic system is shown in Fig 4. For the hydrostatic transmission system, the proposed sliding-mode controller provides a systematic approach to the problem of maintaining stability and consistent performance despite modelling imprecisions like unknown time constants of the actuators. Here, the leakage volume flow q_U and the resulting disturbance torque τ_U are determined by a nonlinear reduced-order disturbance observer and employed for a correction of the inverse dynamics, see Sec. IV. For

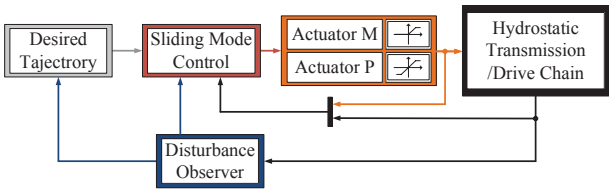

Fig. 4. Block diagram of the observer-based sliding-mode control.

the control design, the the first two time derivatives of the difference pressure and motor angular velocity are calculated. In both cases, the second time derivative depends directly on the control input, leading to a relative degree of four that complies with the system order. By inserting the actuator dynamics, the system dynamics in form of two second-order nonlinear differential equations becomes

$$\begin{aligned} \Delta\ddot{p} &= f_{P1}(\mathbf{x}, \dot{\omega}_P) + \frac{f_{P2}(u_M, \tilde{\alpha}_M)}{T_{uM}} \\ &\quad + \frac{g_P(\omega_P)}{T_{uP}}(u_P - \tilde{\alpha}_P) + d_{P\tau}(\tau_U) + d_{Pq}(\dot{q}_U), \end{aligned} \tag{17}$$

$$\begin{aligned} \ddot{\omega}_M &= f_M(\mathbf{x}, \omega_P) \\ &\quad + \frac{g_M(\Delta p)}{T_{uM}}(u_M - \tilde{\alpha}_M) + d_{M\tau}(\tau_U, \dot{\tau}_U) + d_{Mq}(q_U). \end{aligned} \tag{18}$$

Here, f_{P_1,P_2} and $g_{P,M}$ are nonlinear functions of the system states, whereas $d_{Pi,Mi}$, $i \in \{\tau, q\}$ denote nonlinear functions of the disturbance variables. The vector $\tilde{\mathbf{e}} = [e_P, e_M]$ comprises the tracking error of the difference pressure and the motor angular velocity according to

$$e_P = \Delta p_d - \Delta p, \tag{19}$$

$$e_M = \omega_{Md} - \omega_M. \tag{20}$$

As starting point for the sliding-mode controller, the time-varying switching functions $s_i(t), i \in \{P, M\}$, are defined as follows

$$s_P(t) = \dot{e}_P + 2\lambda e_P + \lambda^2 \int_0^t e_P d\tau, \tag{21}$$

$$s_M(t) = \dot{e}_M + 2\lambda e_M + \lambda^2 \int_0^t e_M d\tau. \tag{22}$$

Here, $\lambda > 0$ is a strictly positive constant. As can be seen from (21) and (22), the dynamics on the sliding surface $s_i(e_i) = 0$ is of second order with respect to the tracking

errors $e_i, i \in \{P, M\}$. Calculating the first time derivatives of $\frac{1}{2}s_i^2, i \in \{P, M\}$, and inserting (17), (18), (21) and (22), results in

$$\begin{aligned}\frac{1}{2}\frac{d}{dt}s_P^2 &= s_P(\ddot{e}_P + 2\lambda\dot{e}_P + \lambda^2 e_P),\\ &= s_P(\Delta\ddot{p}_d + 2\lambda\dot{e}_P + \lambda^2 e_P - f_{P1} - \frac{f_{P2}}{T_{uM}}\\ &\quad - \frac{g_P}{T_{uP}}(u_P - \tilde{\alpha}_P) - d_{P\tau} - d_{Pq}), \end{aligned} \tag{23}$$

$$\begin{aligned}\frac{1}{2}\frac{d}{dt}s_M^2 &= s_M(\ddot{e}_M + 2\lambda\dot{e}_M + \lambda^2 e_M),\\ &= s_M(\ddot{\omega}_{Md} + 2\lambda\dot{e}_M + \lambda^2 e_M - f_M\\ &\quad - \frac{g_M}{T_{uM}}(u_M - \tilde{\alpha}_M) - d_{M\tau} - d_{Mq}). \end{aligned} \tag{24}$$

The following design step consists in determining a control law such that the switching functions according to (21) and (22) converge to zero and remain on the sliding surfaces $s_i(e_i) = 0$ afterwards. This objective is achieved by designing an appropriate control input $u_i, i \in \{P, M\}$, so that the corresponding sliding-condition is satisfied [14]. As a result, the control inputs can be stated as

$$u_P = \frac{\hat{T}_{uP}}{g_P}[\hat{u}_P + \phi_P] + \tilde{\alpha}_P, \tag{25}$$

$$u_M = \frac{\hat{T}_{uM}}{g_M}[\hat{u}_M + \phi_M] + \tilde{\alpha}_M, \tag{26}$$

with

$$\phi_p = \Delta\ddot{p}_d + 2\lambda\dot{e}_P + \lambda^2 e_P - f_{P1} - \frac{f_{P2}}{\hat{T}_{uM}} - d_{P\tau} - d_{Pq}, \tag{27}$$

$$\phi_M = \ddot{\omega}_{Md} + 2\lambda\dot{e}_M + \lambda^2 e_M - f_M - d_{M\tau} - d_{Mq}. \tag{28}$$

Here $\hat{T}_{ui}, i \in \{P, M\}$, represent the estimated actuator time constants. Substituting the designed controller (25) and (26) into (23) and (24) results in

$$\frac{1}{2}\frac{d}{dt}s_P^2 = -\hat{u}_P s_P + \underbrace{\left(\psi_{pP}\frac{\tilde{T}_{uP}}{T_{uP}} + \psi_{pM}\frac{\tilde{T}_{uM}}{T_{uM}}\right)}_{\psi_P} s_P, \tag{29}$$

$$\frac{1}{2}\frac{d}{dt}s_M^2 = -\hat{u}_M s_M + \psi_M\frac{\tilde{T}_{uM}}{\hat{T}_{uM}}s_M, \tag{30}$$

where $\psi_{pP,pM,M}$ are time-varying nonlinear functions. The assumption that the actuator time constants are bounded by

$$0 < T_{i,min} \leq T_i \leq T_{i,max}, \quad i \in \{P, M\} \tag{31}$$

leads to

$$\|\frac{\tilde{T}_{ui}}{T_{ui}}\| \leq T_i, \quad i \in \{P, M\}. \tag{32}$$

By introducing $T_i > 0$, $i \in \{P, M\}$, as positive bounds, the time-varying terms on the right-hand side of the equation (29) and (30), respectively, are also bounded by a positive value

$$\|\psi_i\| T_i \leq F_i, \ i \in \{P, M\}. \tag{33}$$

The switching control action $\hat{u}_i, i \in \{P, M\}$, can be chosen as

$$\hat{u}_i = k_i \mathrm{sgn}(s_i), \quad i \in \{P, M\}, \tag{34}$$

where $k_i = \eta_i + F_i$ denote time-varying but positive gains and $\mathrm{sgn}(s_i)$ represent the sign-functions according to

$$\mathrm{sgn}(s_i) = \begin{cases} 1 & s_i > 0 \\ 0 & s_i = 0 \\ -1 & s_i < 0 \end{cases}, \quad i \in \{P, M\}. \tag{35}$$

By using (34) instead of $\hat{u}_i$ in the equations (29) and (30), a convergence towards the sliding surfaces $s_i = 0$ is achieved in finite time

$$\frac{1}{2}\frac{d}{dt}s_i^2 \leq -\eta_i \mathrm{sgn}(s_i) s_i = -\eta_i |s_i|, \quad i \in \{P, M\}, \tag{36}$$

with constant scalar values η_i, $i \in \{P, M\}$

IV. Nonlinear reduced-order disturbance observer

Disturbance behaviour and tracking accuracy in view of model uncertainties can be significantly improved by introducing a compensating control action provided by a nonlinear reduced-order disturbance observer as described in [15]. The observer design is based on the state equations. The key idea for the observer design is to extend the state equations with an integrator as disturbance model

$$\dot{\mathbf{y}}_m = \mathbf{f}(\mathbf{y}_m, \boldsymbol{\tau}_S, \boldsymbol{\tau}_M) \ , \dot{\boldsymbol{\tau}}_S = \mathbf{0} \ , \tag{37}$$

where $\mathbf{y}_m = [\Delta p, \omega_M]^T$ denotes the measurable difference pressure and motor angular velocity, $\boldsymbol{\tau}_M = [\tilde{\alpha}_P, \tilde{\alpha}_M]^T$ is the vector of the normalised actuator outputs and $\boldsymbol{\tau}_S = [q_U, \tau_U]^T$ represents the vector of system disturbances. The estimated leakage volume flow $\hat{q}_U$ and disturbance torque $\hat{\tau}_U$ follow from

$$\boldsymbol{\tau}_S = \mathbf{H} \cdot \mathbf{y}_m + \mathbf{z}, \tag{38}$$

where $\mathbf{H}$ represents the observer gain matrix. The vector of state equations for $\mathbf{z}$ is given by

$$\dot{\mathbf{z}} = \Phi\left(\mathbf{y}_m, \hat{\boldsymbol{\tau}}_S, \boldsymbol{\tau}_M\right). \tag{39}$$

The observer gain $\mathbf{H} = \mathrm{diag}(h_1, h_2)$ and the vector Φ are chosen such that the steady-state observer error $\tilde{\boldsymbol{\tau}}_S = \boldsymbol{\tau}_S - \hat{\boldsymbol{\tau}}_S$ converges to zero. Thus, Φ can be determined by considering a vanishing steady-state estimation error

$$\dot{\tilde{\boldsymbol{\tau}}}_S = \mathbf{0} = \dot{\boldsymbol{\tau}}_S - \mathbf{H} \cdot \dot{\mathbf{y}}_m - \Phi\left(\mathbf{y}_m, \boldsymbol{\tau}_S - \mathbf{0}, \boldsymbol{\tau}_M\right). \tag{40}$$

In view of $\dot{\boldsymbol{\tau}}_S = \mathbf{0}$, equation (40) yields

$$\begin{aligned}\Phi\left(\mathbf{y}_m, \boldsymbol{\tau}_S - \mathbf{0}, \boldsymbol{\tau}_M\right) &= -\mathbf{H} \cdot \dot{\mathbf{y}}_m\\ &= -\mathbf{H} \cdot \begin{bmatrix} \frac{2q_P}{C_H} - \frac{2q_M}{C_H} - \frac{q_U}{C_H} \\ \\ \frac{-d_V\omega_M}{J_V} + \frac{\tau_M}{J_V} - \frac{\tau_U}{J_V} \end{bmatrix}. \end{aligned} \tag{41}$$

The linearised error dynamics $\dot{\tilde{\boldsymbol{\tau}}}_S$ must be asymptotically stable. All eigenvalues of the Jacobian are, hence, placed in the left complex half-plane according to

$$\frac{\partial \Phi\left(\mathbf{y}_m, \boldsymbol{\tau}_S, \boldsymbol{\tau}_M\right)}{\partial \boldsymbol{\tau}_S} = \begin{bmatrix} \frac{-h_1}{C_H} & 0 \\ 0 & \frac{h_2}{J_V} \end{bmatrix} \stackrel{!}{=} \begin{bmatrix} -s_{B1} & 0 \\ 0 & -s_{B2} \end{bmatrix}, \tag{42}$$

with $s_{B1} > 0$ and $s_{B2} > 0$. This directly leads to the observer gains $h_1 = s_{B1} C_H$ and $h_2 = -s_{B2} J_V$. As depicted in block diagram Fig. 4, disturbance compensation is achieved by substituting the leakage volume flow and the disturbance torque in the sliding-mode control by their estimated values, i.e., $q_U = \hat{q}_U$ and $\tau_U = \hat{\tau}_U$. The asymptotic stability of the closed-loop control system has been investigated thoroughly by simulations.

V. Simulation Results

Taking into account both the measurement noise of the pressure sensors and the quantization effects in the encoder, the tracking performance as well as the steady-state accuracy w.r.t. the motor angular velocity and the difference pressure shall be investigated by simulation. Therefore, the desired trajectories of the pressure difference and motor angular velocity are shown in Fig. 5 as well as their first and second time derivatives.

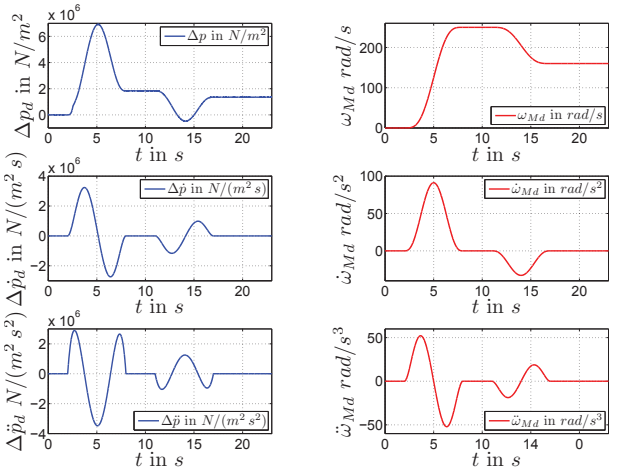

Fig. 5. Desired trajectories for the pressure difference and motor angular velocity.

The desired angular velocity ω_{Md} is formulated by a $7th$ order polynomial, and the desired trajectory of Δp_d is calculated with a desired value for the normalized motor input $u_{Md} = 0.8$, which can be adapted to the given drive situation. This leads to the following relationships for Δp_d and the first two time derivatives

$$\Delta p_d = \frac{J_V \dot{\omega}_{Md} + d_V \omega_{Md} + \hat{\tau}_U}{0.8 \tilde{V}_M}, \tag{43}$$

$$\Delta \dot{p}_d = \frac{J_V \ddot{\omega}_{Md} + d_V \dot{\omega}_{Md} + \dot{\hat{\tau}}_U}{0.8 \tilde{V}_M}, \tag{44}$$

$$\Delta \ddot{p}_d = \frac{J_V \dddot{\omega}_{Md} + d_V \ddot{\omega}_{Md} + \ddot{\hat{\tau}}_U}{0.8 \tilde{V}_M}. \tag{45}$$

Note that Δp_d depends on both ω_{Md} and estimated disturbance $\hat{\tau}_U$. The disturbance torque that is employed in the simulation consists of two terms: 1) a static nonlinear friction model and 2) a vehicle mass increased by 10%. In the implementation, the time derivatives of τ_U, $\dot{\hat{\tau}}_U$ and $\ddot{\hat{\tau}}_U$, are neglected in the equations (44) and (45). The estimation results concerning the disturbance torque shown in Fig. 6 (upper part) are quite good and, hence, used for a disturbance compensation. The same holds for the estimated leakage volume flow (proportional to difference pressure), which is shown in Fig. 6 (lower part).

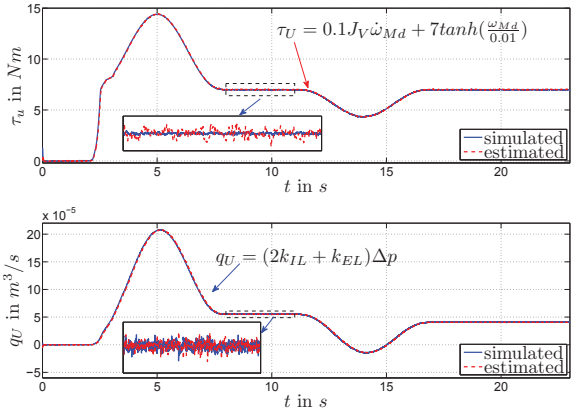

Fig. 6. Estimation of the considered disturbance torque (upper part) and leakage volume flow (lower part).

Fig. 7 depicts the tracking performance regarding the difference pressure and the motor angular velocity as well as the tracking errors with only imperfectly known time constants (-50 % deviation from their nominal values) in the actuator dynamics. It indicates that the sliding-mode controller with the disturbance observer works quite well in the case of uncertainty in the actuator dynamics: the motor angular velocity is tracked with an error bounded by 0.5 rad/s, whereas the error of the difference pressure is bounded by 0.03 bar. Fig. 8 shows the corresponding normalized tilt angles of the hydraulic pump and motor $\tilde{\alpha}_i$, $i \in \{P, M\}$

The estimated leakage volume flow and tracking errors depicted in Fig. 9 emphasise that the combination of the sliding-mode controller and the observer-based disturbance compensation guarantees an outstanding tracking performance despite an unexpected additional leakage. This additional leakage oil flow could be caused by a pressure relief valve that is not perfectly closed.

VI. Conclusions

In this paper, a sliding-mode trajectory tracking control in combination with a disturbance observer is presented for a hydrostatic transmission with uncertainties. The modelling of this mechatronic system leads to a system of four nonlinear differential equations. Two sources of model uncertainty are considered in the paper: 1) unknown time constants in the actuator dynamics and 2) unknown disturbances in form of a leakage volume flow and a disturbance torque acting

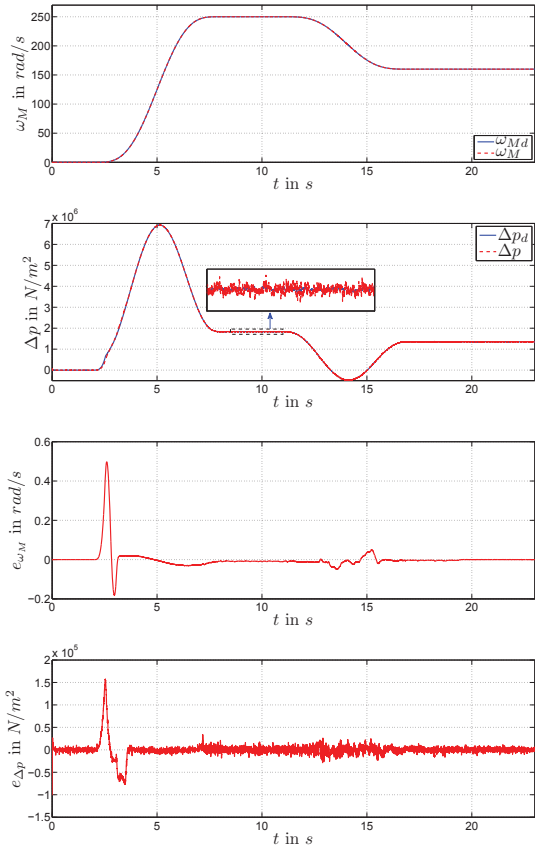

Fig. 7. Tracking performance using sliding-mode control for the hydrostatic drive train with only imperfectly known time constants in the actuator dynamics.

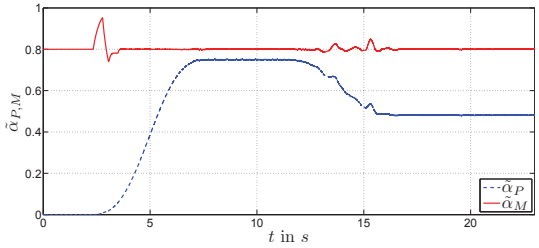

Fig. 8. Normalised tilt angles of both the hydraulic pump and the motor.

on the hydraulic motor. Reasonable assumptions on the boundedness of the time constants in the actuator dynamics enables to select proper gains for the sliding-mode control. The control approach guarantees the robust stability of the closed-loop system. The simulation results show that the proposed control leads to a high tracking performance even in the case of imperfect knowledge of the actuator dynamics.

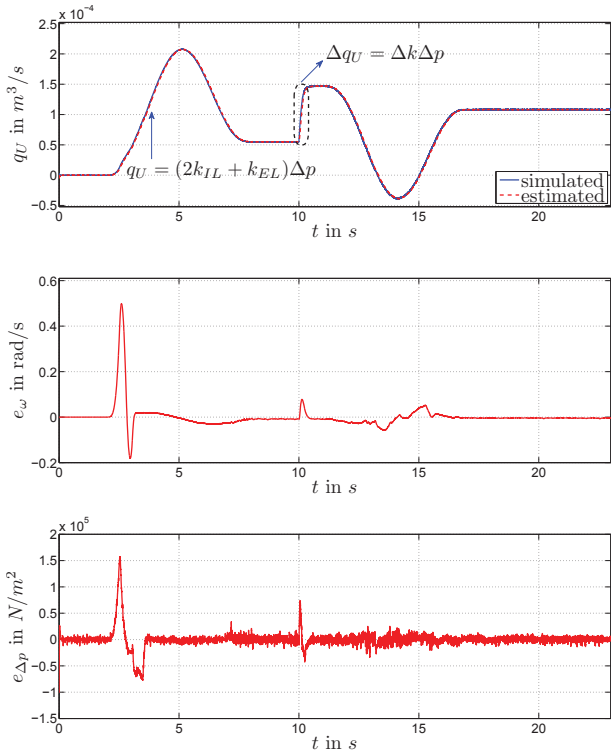

Fig. 9. Estimation of the leakage volume flow with an additional leakage at 4.5 s as well as the corresponding tracking errors of motor angular velocity and difference pressure.

References

[1] M. Jelali and A. Kroll, *Hydraulic Servo-systems: Modelling, Identification and Control*. London, UK: Springer-Verlag, 2003.

[2] N. Diepeveen and A. Laguna, "Dynamics modelling of fluid power transmissions for wind turbine," in *EWEA Offshore (2011)*, Amsterdam, Netherland, 2011.

[3] B. Dolan and H. Aschemann, "Control of a wind turbine with a hydrostatic transmission - an extended linearisation approach," in *17th International Conference on Methods and Models in Automation and Robotics (MMAR) (2012)*, Miedzyzdroje, Poland, 27-30 Aug 2012, pp. 445–450.

[4] A. Pusha, A. Izadian, S. Hamzehlouia, N. Girrens, and S. Anwar, "Modelling of gearless wind power transfer," in *IECON 2011-37th Annual Conference on IEEE Industrial Electronics Society*, 7-10 Nov 2011, pp. 3176–3179.

[5] S. Stoll, M. Kliffken, M. Behm, and X. Wang, "Regelungskonzepte für hydrostatische Antriebe in mobilen Arbeitsmaschinen (in German)," *at – Automatisierungstechnik*, p. 5 (2007) 2, 19-21 Aug. 2007.

[6] H. Aschemann, J. Ritzke, and H. Schulte, "Model-based nonlinear trajectory control of a drive chain with hydrostatic transmission," in *14th International Conference on Methods and Models in Automation and Robotics (2009)*, vol. 14, Miedzyzdroje, Poland, 19-21 Aug. 2009.

[7] J. Ritzke and H. Aschemann, "Design and experimental validation of nonlinear trajectory control of a drive chain with hydrostatic transmission," in *12th Scandinavian International Conference on Fluid Power*, Tampere, Finland, 18-21 May 2011.

[8] A. Koshkouei, K. Burnham, and A. Zinober, "Dynamic Sliding Mode Control Design," in *IEE Proc.-Control Theory Appl.*, vol. 152 No.4, July. 2005.

[9] J.-J. E. Slotine and W. Li., *Applied Nonlinear Control*. Prentice Hall, 1991.

[10] K. D. Yang, V. I. Utkin, and U. Özgüner., "A Control Engineer's Guide to Sliding Mode Control." in *IEEE Transactions on Control Systems Technology.*, vol. 7 No.3, May. 1999.

[11] H. Schulte, "Control-oriented modelling of hydrostatic transmissions using Takagi-Sugeno fuzzy systems," in *IEEE International Conference on Fuzzy Systems (2007)*, London, UK, 2007, pp. 2030–2035.

[12] A. Kugi, K. Schlacher, H. Aitzetmueller, and G. Hirmann, "Modelling and simulation of a hydrostatic transmission with variable-displacement pump," *Mathematics and Computers in Simulation*, vol. 53, pp. 409–414, 2000.

[13] P. Rohner, *Industrial Hydraulic Control: A Textbook for Fluid Power Technicians*. John Wiley & Sons, 2004.

[14] J. E. Slotine and W. Li, *Applied Nonlinear Control*. Prentice Hall, 1991.

[15] B. Friedland, *Advanced Control System Design*. Prentice Hall, 1996.